Selective Smoothed Finite Element Method

T. T. Nguyen[1,**], G. R. Liu[1,2], K. Y. Dai[1,2], K. Y. Lam[3]

1. Center for Advanced Computations in Engineering Science, Department of Mechanical Engineering,
National University of Singapore, 9 Engineering Drive 1, Singapore 117576, Singapore;
2. Singapore-MIT Alliance (SMA), E4-04-10, 4 Engineering Drive 3, Singapore 117576, Singapore;
3. School of Mechanical and Aerospace Engineering, Nanyang Technological University,
50 Nanyang Avenue, Singapore 639798, Singapore

Abstract: The paper examines three selective schemes for the smoothed finite element method (SFEM) which was formulated by incorporating a cell-wise strain smoothing operation into the standard compatible finite element method (FEM). These selective SFEM schemes were formulated based on three selective integration FEM schemes with similar properties found between the number of smoothing cells in the SFEM and the number of Gaussian integration points in the FEM. Both scheme 1 and scheme 2 are free of nearly incompressible locking, but scheme 2 is more general and gives better results than scheme 1. In addition, scheme 2 can be applied to anisotropic and nonlinear situations, while scheme 1 can only be applied to isotropic and linear situations. Scheme 3 is free of shear locking. This scheme can be applied to plate and shell problems. Results of the numerical study show that the selective SFEM schemes give more accurate results than the FEM schemes.

Key words: finite element method (FEM); smoothed finite element method (SFEM); strain smoothing; smoothing cell; selective

Introduction

In the finite element method (FEM), standard lower-order quadrilateral isoparametric elements are the most popular and widely used for solving elasticity problems. However, they have two serious drawbacks: (1) They are overly stiff in bending problems due to the shear locking phenomenon; (2) They lock in nearly incompressible problems when the bulk modulus becomes infinite. To overcome these drawbacks, the reduced integration technique has been used, which saves a great deal of computational cost due to the use of only one point at the element centroid to evaluate

the stiffness matrix instead of four integration points. This technique was devised by Zienkiewicz et al.[1] to alleviate shear locking in plate and shell bending. This technique was also shown to provide the added benefit of eliminating spurious constraints in incompressible applications, as demonstrated by Malkus and Hughes[2]. Unfortunately, in most cases reduced integration leads to artificial zero energy modes, precluding general application of this method. In many cases, selective reduced integration establishes a good compromise between efficiency (avoiding locking) and stability (avoiding artificial zero energy modes). The idea is to split the strain energy into individual parts and apply different integration rules to evaluate the corresponding contributions to the stiffness matrix.

So far, three selective reduced integration schemes are widely used. The first scheme (S1) and the second

scheme (S2) are used to overcome the incompressible locking[3]. The idea of the first scheme is to decompose the material properties matrix into two parts, the volumetric part and non-volumetric part, and the stiffness matrix is also decomposed into two parts correspondingly. Then, the reduced integration is used only on the volume-part and the full Gauss integration is used on the remaining-part. However, in general, anisotropic and/or nonlinear situations, an explicit segregation of the contributions to the matrix equations into volumetrically stiff and non-volumetric terms as the scheme 1 is not always apparent. This limits the generality of scheme 1. In principle, a decomposition of the material tangent stiffness into dilatational, deviatoric, and dilatational-deviatoric coupling terms may always be achieved. Hughes[3,4] generalized the selective integration procedures to anisotropic and nonlinear media in the B-bar method, which is referred to in this paper as the second selective integration scheme (S2). The idea of this scheme is to improve the dilatational part of the strain-displacement matrix by using reduced integration and the full Gauss integration is still used to calculate the stiffness matrix from the "improved" strain-displacement matrix. The third scheme (S3) is used to overcome the shear locking phenomenon in bending problems[1]. Reduced integration is used for the shear part and full integration for the remaining parts in calculating the stiffness matrix.

To overcome these problems in the FEM, Liu et al.[5,6] proposed, for the first time, a smoothed finite element method (SFEM) by combining the existing FEM technology and the strain smoothing technique of meshfree methods. In this method, elements are used as in the FEM with smoothing operations performed over the elements. Depending on the accuracy and stability requirements, an element may be further subdivided into several smoothing cells with the smoothing operations then performed on each smoothing cell within an element. The Galerkin weak form is used as in the FEM, but the smoothed strains are used for computing the stiffness matrix. With a constant smoothing function, area integrations over the cell in the weak form become line integrations along the cell boundaries. Hence, no derivatives of the shape functions are involved in computing the field gradients to

form the stiffness matrix. Numerical studies have demonstrated that the SFEM has some advantages over the standard FEM using 4-node isoparametric elements. For example, (1) The SFEM gives better results than the FEM in both displacement and energy because the SFEM stiffness is less than that of the FEM; (2) The domain discretization in the SFEM is more flexible than in the FEM so even severe distorted, tile or polygonal elements can be used; (3) The field gradients are computed directly using only the shape functions themselves; (4) The construction of shape functions can be much easier than in the FEM, which practically allows explicit interpolations of field variables; and (5) Many existing FEM algorithms can be easily modified and incorporated into the SFEM. Most importantly, these good features are gained without increasing the effort in both modeling and computation, and the changes to existing FEM codes are very minimal. All these features have been demonstrated in detail by Liu et al.[5,6] using many numerical examples and various complex elements including extremely distorted quadrilateral elements, polygon, and tile elements. However, the problems relating to incompressible and shear locking phenomena have not yet been studied and effective SFEM schemes to solve these problems have not yet been established.

This paper presents three selective SFEM schemes to solve the problems of incompressible and shear locking. The three selective schemes are formulated based on the three selective integration FEM schemes with similar properties found between the number of smoothing cells in the SFEM and the number of Gaussian integration points in the FEM.

1 Smoothed Finite Element Method

1.1 Finite element method[3,7-9]

The discrete equations for the finite element method are generated from the Galerkin weak form

$$\int_{\Omega} (\nabla_S \delta \boldsymbol{u})^{\mathrm{T}} \boldsymbol{D} (\nabla_S \boldsymbol{u}) \mathrm{d}\Omega - \int_{\Omega} (\delta \boldsymbol{u})^{\mathrm{T}} \boldsymbol{b} \mathrm{d}\Omega -$$

$$\int_{\Gamma_t} (\delta \boldsymbol{u})^{\mathrm{T}} \bar{\boldsymbol{t}} \mathrm{d}\Gamma = 0 \qquad (1)$$

where $\boldsymbol{D}$ is the material property matrix, $\boldsymbol{u} \in H^1(\Omega)$

are trial functions, and $\delta u \in H_0^1(\Omega)$ are test functions. Here $H^1(\Omega)$ denotes the Sobolev space of functions with square integrable derivatives in Ω and $H_0^1(\Omega)$ is the subset of $H^1(\Omega)$ with vanishing values on Γ_u. The FEM uses the following trial and test functions:

$$u^{\mathrm{h}}(x) = \sum_{I=1}^{\mathrm{NP}} N_I(x) d_I \,,$$

$$\delta u^{\mathrm{h}}(x) = \sum_{I=1}^{\mathrm{NP}} N_I(x) \delta d_I \quad (2)$$

where NP is the number of nodes in the element, $d_I = \begin{bmatrix} u_I & v_I \end{bmatrix}^{\mathrm{T}}$ is the nodal displacement vector, and $N_I(x) = \begin{bmatrix} N_I(x) & 0 \\ 0 & N_I(x) \end{bmatrix}$ is the shape function matrix which satisfies the conditions

$$N_I(x_J) = \delta_{IJ}, \quad \sum_{I=1}^{\mathrm{NP}} N_I(x) = 1 \quad (3)$$

where δ_{IJ} is the Kronecker delta.

By substituting the approximations u^{h} and δu^{h} into the weak form and invoking the arbitrariness of virtual nodal displacements, Eq. (1) can be written as the standard discretized algebraic system of equations

$$K^{\mathrm{FEM}} d = f \quad (4)$$

where K^{FEM} is the stiffness matrix and f is the element force vector with entries of

$$K_{IJ}^{\mathrm{FEM}} = \int_{\Omega} B_I^{\mathrm{T}} D B_J \mathrm{d}\Omega \quad (5)$$

$$f_I = \int_{\Omega} N_I^{\mathrm{T}}(x) b \mathrm{d}\Omega + \int_{\Gamma_t} N_I^{\mathrm{T}}(x) \bar{t} \mathrm{d}\Gamma \quad (6)$$

with the strain matrix defined as

$$B_I(x) = \nabla_S N_I(x) = \begin{bmatrix} \dfrac{\partial N_I(x)}{\partial x} & 0 \\ 0 & \dfrac{\partial N_I(x)}{\partial y} \\ \dfrac{\partial N_I(x)}{\partial y} & \dfrac{\partial N_I(x)}{\partial x} \end{bmatrix} \quad (7)$$

1.2 Smoothed finite element method[5,6]

The SFEM combines the standard FEM procedure with a strain smoothing operation. SFEM uses elements as in the FEM with smoothing operations performed over the smoothing cells. The final discretized algebraic system of equations has the form

$$K^{\mathrm{SFEM}} d = f \quad (8)$$

where K^{SFEM} is the smoothed stiffness matrix given by

$$K_{IJ}^{\mathrm{SFEM}} = \sum_{C=1}^{\mathrm{SC}} \int_{\Omega_C} \tilde{B}_{CI}^{\mathrm{T}} D \tilde{B}_{CJ} \mathrm{d}\Omega = \sum_{C=1}^{\mathrm{SC}} \tilde{B}_{CI}^{\mathrm{T}} D \tilde{B}_{CJ} A_C \quad (9)$$

where $A_C = \int_{\Omega_C} \mathrm{d}\Omega$ is the smoothing cell area Ω_C, SC is the number of smo $\Omega = \Omega_1 \cup \Omega_2 \cup \cdots \cup \Omega_{\mathrm{SC}}$ othing cells in element Ω such that and $\Omega_1 \cap \Omega_2 \cap \cdots \cap \Omega_{\mathrm{SC}} = \varnothing$, and $\tilde{B}_{CI}$ is the smoothed strain matrix obtained by the following strain smoothing operation:

$$\tilde{\varepsilon}_C^{\mathrm{h}} = \int_{\Omega_C} \varepsilon^{\mathrm{h}}(x) \Phi_C(x) \mathrm{d}\Omega \quad (10)$$

where $\varepsilon^{\mathrm{h}}(x) = \nabla_S u^{\mathrm{h}}(x)$ is the strain obtained from the displacement with compatibility and $\Phi_C(x)$ is a given smoothing function that satisfies at least the unity property

$$\int_{\Omega_C} \Phi_C(x) \mathrm{d}\Omega = 1 \quad (11)$$

The following constant smoothing function

$$\Phi_C(x) = \begin{cases} 1/A_C, & x \in \Omega_C; \\ 0, & x \notin \Omega_C \end{cases} \quad (12)$$

and the divergence theorem can be used to get the smoothed strain in the domain Ω_C

$$\tilde{\varepsilon}_C^{\mathrm{h}} = \int_{\Omega_C} \nabla_S u^{\mathrm{h}}(x) \frac{1}{A_C} \mathrm{d}\Omega = \frac{1}{A_C} \int_{\Omega_C} \nabla_S u^{\mathrm{h}}(x) \mathrm{d}\Omega =$$

$$\frac{1}{A_C} \int_{\Gamma_C} n_C(x) u^{\mathrm{h}}(x) \mathrm{d}\Gamma \quad (13)$$

where Γ_C is the boundary of the domain Ω_C and $n_C(x)$ is the outward normal vector on the boundary Γ_C.

Substitution of Eq. (2) into Eq. (13) gives the smoothed strain as

$$\tilde{\varepsilon}_C^{\mathrm{h}} = \sum_{I=1}^{\mathrm{NP}} \tilde{B}_{CI} d_I \quad (14)$$

where the smoothed strain matrix $\tilde{B}_{CI}$ is

$$\tilde{\boldsymbol{B}}_{CI} = \frac{1}{A_C} \int_{\Gamma_c} N_I(\boldsymbol{x}) \boldsymbol{n}_C(\boldsymbol{x}) \mathrm{d}\Gamma =$$

$$
\begin{bmatrix}
\frac{1}{A_C} \int_{\Gamma_c} N_I(\boldsymbol{x}) n_{Cx}(\boldsymbol{x}) \mathrm{d}\Gamma & 0 \\[2mm]
0 & \frac{1}{A_C} \int_{\Gamma_c} N_I(\boldsymbol{x}) n_{Cy}(\boldsymbol{x}) \mathrm{d}\Gamma \\[2mm]
\frac{1}{A_C} \int_{\Gamma_c} N_I(\boldsymbol{x}) n_{Cy}(\boldsymbol{x}) \mathrm{d}\Gamma & \frac{1}{A_C} \int_{\Gamma_c} N_I(\boldsymbol{x}) n_{Cx}(\boldsymbol{x}) \mathrm{d}\Gamma
\end{bmatrix}
$$

$$\tag{15}$$

The SFEM has been proven to be energy consistent with very nice monotonic convergence properties[6].

2 Three Selective SFEM Schemes

Liu et al.[5,6] theoretically and numerically showed that the solution of SFEM with one smoothing cell (SC=1) has similar properties to the FEM using reduced integration. The element stiffness matrix will contain spurious zero energy modes and the global stiffness matrix can still be singular after imposing essential boundary conditions depending on the problem. SFEM solutions with more than one smoothing cell (SC>1) can avoid spurious modes and give stable results. This property is quite similar to that of the FEM using full Gauss integration. Hence, the similarities enable easy application of all three schemes of selective integration for the FEM (S1, S2, and S3) into the SFEM. The advantage of the SFEM is that it has more choices than the FEM in choosing the number of smoothing cells being larger than one (SC>1). In this paper, four smoothing cells will be used mainly to simplify the analysis.

2.1 Scheme 1

This scheme does not experience incompressible locking[3]. The material property matrix $\boldsymbol{D}$ for isotropic materials may be written as

$$\boldsymbol{D} = \bar{\boldsymbol{D}} + \bar{\bar{\boldsymbol{D}}} \tag{16}$$

where $\bar{\boldsymbol{D}}$ is the μ-part of $\boldsymbol{D}$ and $\bar{\bar{\boldsymbol{D}}}$, the remainder, is the λ-part, in which μ is the shearing modulus, $\lambda = \dfrac{2\nu\mu}{1-2\nu}$ is Lame's parameter, and ν is Poisson ratio.

Specifically, the material property matrices for various problems are written as follows.

For plane strain,

$$
\boldsymbol{D} =
\begin{bmatrix}
\lambda + 2\mu & \lambda & 0 \\
\lambda & \lambda + 2\mu & 0 \\
0 & 0 & \mu
\end{bmatrix}
= \mu
\begin{bmatrix}
2 & 0 & 0 \\
0 & 2 & 0 \\
0 & 0 & 1
\end{bmatrix}
+
$$
$$
\lambda
\begin{bmatrix}
1 & 1 & 0 \\
1 & 1 & 0 \\
0 & 0 & 0
\end{bmatrix}
= \bar{\boldsymbol{D}} + \bar{\bar{\boldsymbol{D}}} \tag{17}
$$

where

$$
\bar{\boldsymbol{D}} = \mu
\begin{bmatrix}
2 & 0 & 0 \\
0 & 2 & 0 \\
0 & 0 & 1
\end{bmatrix}, \quad
\bar{\bar{\boldsymbol{D}}} = \lambda
\begin{bmatrix}
1 & 1 & 0 \\
1 & 1 & 0 \\
0 & 0 & 0
\end{bmatrix}.
$$

For axis-symmetric geometries,

$$
\boldsymbol{D} = \mu
\begin{bmatrix}
2 & 0 & 0 & 0 \\
0 & 2 & 0 & 0 \\
0 & 0 & 1 & 0 \\
0 & 0 & 0 & 2
\end{bmatrix}
+ \lambda
\begin{bmatrix}
1 & 1 & 0 & 1 \\
1 & 1 & 0 & 1 \\
0 & 0 & 0 & 0 \\
1 & 1 & 0 & 1
\end{bmatrix}
= \bar{\boldsymbol{D}} + \bar{\bar{\boldsymbol{D}}} \tag{18}
$$

For three-dimensional geometries,

$$
\boldsymbol{D} = \mu
\begin{bmatrix}
2 & & & & & \\
& 2 & & & & \\
& & 2 & & & \\
& & & 1 & & \\
& & & & 1 & \\
& & & & & 1
\end{bmatrix}
+ \lambda
\begin{bmatrix}
1 & 1 & 1 & 0 & 0 & 0 \\
1 & 1 & 1 & 0 & 0 & 0 \\
1 & 1 & 1 & 0 & 0 & 0 \\
0 & 0 & 0 & 0 & 0 & 0 \\
0 & 0 & 0 & 0 & 0 & 0 \\
0 & 0 & 0 & 0 & 0 & 0
\end{bmatrix}
=
$$
$$
\bar{\boldsymbol{D}} + \bar{\bar{\boldsymbol{D}}} \tag{19}
$$

Using Eq. (16) in Eq. (9) gives

$$\boldsymbol{K}_{IJ}^{\mathrm{SFEM}} = \bar{\boldsymbol{K}}_{IJ}^{\mathrm{SFEM}} + \bar{\bar{\boldsymbol{K}}}_{IJ}^{\mathrm{SFEM}} \tag{20}$$

where

$$\bar{\boldsymbol{K}}_{IJ}^{\mathrm{SFEM}} = \sum_{C=1}^{\mathrm{SC}} \tilde{\boldsymbol{B}}_{CI}^{\mathrm{T}} \bar{\boldsymbol{D}} \tilde{\boldsymbol{B}}_{CJ} A_C \tag{21}$$

$$\bar{\bar{\boldsymbol{K}}}_{IJ}^{\mathrm{SFEM}} = \sum_{C=1}^{\mathrm{SC}} \tilde{\boldsymbol{B}}_{CI}^{\mathrm{T}} \bar{\bar{\boldsymbol{D}}} \tilde{\boldsymbol{B}}_{CJ} A_C \tag{22}$$

Selective smoothing (first scheme, S1) refers to the use of SC=1 only on $\bar{\bar{\boldsymbol{D}}}$ (related to the λ term), and SC>1 on $\bar{\boldsymbol{D}}$ (related to the μ term). Uniform smoothing refers to the use of SC=1 on both $\bar{\boldsymbol{D}}$ and $\bar{\bar{\boldsymbol{D}}}$ for uniform smoothing.

With scheme 1, the SFEM solution has the following properties:

(1) Ensure reduction of the stiffness matrix $\boldsymbol{K}_{IJ}^{\mathrm{SFEM}}$ of the element. Since $\lambda/\mu \gg 1$, $\bar{\bar{\boldsymbol{K}}}_{IJ}^{\mathrm{SFEM}}$ is propor-

tional to λ, and $\overline{K}_{IJ}^{\text{SFEM}}$ is proportional to μ, the numerical values of the terms in $\overline{\overline{K}}_{IJ}^{\text{SFEM}}$ tend to be very large compared with those in $\overline{K}_{IJ}^{\text{SFEM}}$. Therefore, when using SC=1 for $\overline{\overline{K}}_{IJ}^{\text{SFEM}}$, the stiffness matrix K_{IJ}^{SFEM} is considerably reduced.

(2) The rank of the stiffness matrix is ensured correctly. The disadvantage of uniform smoothing is that the rank of the element stiffness may be reduced, resulting in singularity of the global matrix. Selective smoothing retains the correct rank of the element stiffness; therefore, the global stiffness also possesses the correct rank. This follows from the fact that $\overline{K}_{IJ}^{\text{SFEM}}$ is positive definite, so $\overline{\overline{K}}_{IJ}^{\text{SFEM}}$ does not need to be considered when determining the rank of the entire stiffness matrix.

(3) Selective smoothing is effective for nearly incompressible cases. $\overline{\overline{K}}_{IJ}^{\text{SFEM}}$ is the part of the stiffness matrix that describes the volumetrically stiff behavior. Hence, SFEM with SC>1 tends toward incompressible locking. Hence, the use of SC=1 with $\overline{\overline{K}}_{IJ}^{\text{SFEM}}$ will alleviate this tendency.

2.2 Scheme 2

The second scheme, also called the B-bar approach[3,4], is for handling problems with nearly incompressible locking for anisotropic and/or nonlinear situations.

The strain-displacement matrix of a smoothing cell of an element may be expanded in terms of nodal sub-matrices as

$$\tilde{B}_C = \begin{bmatrix} \tilde{B}_{C1} & \tilde{B}_{C2} & \dots & \tilde{B}_{\text{CNP}} \end{bmatrix} \quad (23)$$

where $1 \leqslant C \leqslant \text{SC}$. In three-dimensional analyses, a typical sub-matrix, $\tilde{B}_{Ca}$, $1 \leqslant a \leqslant \text{NP}$, can be written as

$$\tilde{B}_{Ca} = \begin{bmatrix} \tilde{B}_{C1} & 0 & 0 \\ 0 & \tilde{B}_{C2} & 0 \\ 0 & 0 & \tilde{B}_{C3} \\ 0 & \tilde{B}_{C3} & \tilde{B}_{C2} \\ \tilde{B}_{C3} & 0 & \tilde{B}_{C1} \\ \tilde{B}_{C2} & \tilde{B}_{C1} & 0 \end{bmatrix} \quad (24)$$

in which

$$\tilde{B}_{Ci} = \int_{\Omega_C} \frac{1}{A_C} \frac{\partial N_a}{\partial x_i} \, \mathrm{d}\Omega = \frac{1}{A_C} \int_{\Gamma_C} N_a n_{x_i} \, \mathrm{d}\Gamma,$$

$$1 \leqslant i \leqslant 3 \quad (25)$$

where N_a is the shape function associated with node a and x_i is the i-th Cartesian coordinate.

These are the standard expressions, but they must be modified to be successfully applied to volumetrically stiff materials. Let $\tilde{B}_{Ca}^{\text{dil}}$ denote the dilatational part of $\tilde{B}_{Ca}$, i.e.

$$\tilde{B}_{Ca}^{\text{dil}} = \frac{1}{3} \begin{bmatrix} \tilde{B}_{C1} & \tilde{B}_{C2} & \tilde{B}_{C3} \\ \tilde{B}_{C1} & \tilde{B}_{C2} & \tilde{B}_{C3} \\ \tilde{B}_{C1} & \tilde{B}_{C2} & \tilde{B}_{C3} \\ 0 & 0 & 0 \\ 0 & 0 & 0 \\ 0 & 0 & 0 \end{bmatrix} \quad (26)$$

The deviatoric part of $\tilde{B}_{Ca}$ is then defined as

$$\tilde{B}_{Ca}^{\text{dev}} = \tilde{B}_{Ca} - \tilde{B}_{Ca}^{\text{dil}} \quad (27)$$

To achieve an effective formulation for nearly-incompressible applications, $\tilde{B}_{Ca}^{\text{dil}}$ needs to be replaced by an "improved" dilatational contribution, denoted by

$$\overline{B}_{Ca}^{\text{dil}} = \frac{1}{3} \begin{bmatrix} \overline{B}_{C1} & \overline{B}_{C2} & \overline{B}_{C3} \\ \overline{B}_{C1} & \overline{B}_{C2} & \overline{B}_{C3} \\ \overline{B}_{C1} & \overline{B}_{C2} & \overline{B}_{C3} \\ 0 & 0 & 0 \\ 0 & 0 & 0 \\ 0 & 0 & 0 \end{bmatrix} \quad (28)$$

$\overline{B}_{Ca}^{\text{dil}}$ will be calculated using SC=1. This is quite similar to the use of the mean value of $\tilde{B}_{Ci}$ to calculate the dilatational contribution in the scheme 2. In place of $\tilde{B}_{Ca}$ now employ

$$\overline{B}_{Ca} = \tilde{B}_{Ca}^{\text{dev}} + \overline{B}_{Ca}^{\text{dil}} \quad (29)$$

Finally, the normal SFEM procedure (SC>1) is used to calculate the stiffness matrix.

A modified B-Bar method for plane strain can be developed by modifying the standard B-Bar method which satisfies the $\tilde{\varepsilon}_z = 0$ condition only in the weak sense. To exactly satisfy $\tilde{\varepsilon}_z = 0$ at any point within the element, the B-Bar method can be constructed by replacing the $\tilde{B}_{Ca}^{\text{dil}}$ matrix by a $\tilde{B}_{Ca}^{\text{mean}}$ matrix[10],

$$\tilde{B}_{Ca}^{\text{mean}} = \begin{bmatrix} \dfrac{1}{2}\tilde{B}_{C1} & \dfrac{1}{2}\tilde{B}_{C2} \\[2mm] \dfrac{1}{2}\tilde{B}_{C1} & \dfrac{1}{2}\tilde{B}_{C2} \\[2mm] 0 & 0 \end{bmatrix} \tag{30}$$

which corresponds to use of a "modified" mean strain $\tilde{\varepsilon}_{\text{m}}^* = \dfrac{1}{2}\left(\tilde{\varepsilon}_x + \tilde{\varepsilon}_y\right)$ instead of the standard mean strain $\tilde{\varepsilon}_{\text{m}} = \dfrac{1}{3}\left(\tilde{\varepsilon}_x + \tilde{\varepsilon}_y + \tilde{\varepsilon}_z\right)$.

2.3 Scheme 3

The third scheme is for dealing with shear locking[1]. The solution of plate and shell problems by independent specification of slopes and middle surface displacements is attractive due to its simplicity and its ability to reproduce shear deformation. Unfortunately, elements of this type become much too stiff as the thickness is reduced.

With the SFEM, one way to obtain a suitable improved flexibility is simply to use the different smoothing schemes for the individual components of the integrand of the stiffness matrix. The use of SC>1 for the "bending" and "membrane" parts (for the shell) and SC=1 for the "shear" part leads to a formulation which is free from shear locking without hurting convergence properties.

(1) For the plate problem[11]

Depending on the FEM formulation, the SFEM expression to compute the stiffness matrix for a standard plate element is

$$K_{\text{a}} = \left(\frac{h^3}{12} \sum_{C=1}^{\text{SC}} \int_{\Omega_C} \tilde{B}_{Cb}^{\text{T}} D_{\text{b}} \tilde{B}_{Cb} \, \text{d}\Omega \right) + \kappa h \int_{\Omega_e} \tilde{B}_{\text{s}}^{\text{T}} D_{\text{s}} \tilde{B}_{\text{s}} \, \text{d}\Omega \tag{31}$$

where

$$\tilde{B}_{CbI} = \frac{1}{A_C} \begin{bmatrix} \displaystyle\int_{\Gamma_C} N_I(\boldsymbol{x}) n_{Cx}(\boldsymbol{x}) \text{d}\Gamma & 0 & 0 \\[4mm] 0 & \displaystyle\int_{\Gamma_C} N_I(\boldsymbol{x}) n_{Cy}(\boldsymbol{x}) \text{d}\Gamma & 0 \\[4mm] \displaystyle\int_{\Gamma_C} N_I(\boldsymbol{x}) n_{Cy}(\boldsymbol{x}) \text{d}\Gamma & \displaystyle\int_{\Gamma_C} N_I(\boldsymbol{x}) n_{Cx}(\boldsymbol{x}) \text{d}\Gamma & 0 \end{bmatrix} \tag{32}$$

$$\tilde{B}_{sI} = \begin{bmatrix} -N_I(\boldsymbol{x}) & 0 & \dfrac{1}{A_e} \displaystyle\int_{\Gamma_e} N_I(\boldsymbol{x}) n_x(\boldsymbol{x}) \text{d}\Gamma \\[4mm] 0 & -N_I(\boldsymbol{x}) & \dfrac{1}{A_e} \displaystyle\int_{\Gamma_e} N_I(\boldsymbol{x}) n_y(\boldsymbol{x}) \text{d}\Gamma \end{bmatrix} \tag{33}$$

$$D_{\text{b}} = \frac{E}{1-\nu^2} \begin{bmatrix} 1 & \nu & 0 \\ \nu & 1 & 0 \\ 0 & 0 & \dfrac{1-\nu}{2} \end{bmatrix}$$

and

$$D_{\text{s}} = \begin{bmatrix} \mu & 0 \\ 0 & \eta \end{bmatrix} \tag{34}$$

(2) For the shell problem (shells made of in-plane and bending elements)[11]

The shell element stiffness matrix is given by

$$\begin{bmatrix} K_{\text{b}} & 0 \\ 0 & K_{\text{m}} \end{bmatrix} \begin{Bmatrix} d_{\text{b}} \\ d_{\text{m}} \end{Bmatrix} = \begin{Bmatrix} F_{\text{b}} \\ F_{\text{m}} \end{Bmatrix} \tag{35}$$

where K indicates the stiffness matrix, d indicates the general nodal displacement vector, and F indicates the general nodal force vector. The matrices and vectors consist a plate bending part and a plate stretching part. Subscripts b and m denote bending and membrane (stretching) deformations of the shell element.

$$K_{\text{b}} = \left(\frac{h^3}{12} \sum_{C=1}^{\text{SC}} \int_{\Omega_C} \tilde{B}_{Cb}^{\text{T}} D_{\text{b}} \tilde{B}_{Cb} \, \text{d}\Omega \right) + \kappa h \int_{\Omega_e} \tilde{B}_{\text{s}}^{\text{T}} D_{\text{s}} \tilde{B}_{\text{s}} \, \text{d}\Omega \tag{36}$$

$$K_{\text{m}} = h \sum_{C=1}^{\text{SC}} \int_{\Omega_C} \tilde{B}_{Cm}^{\text{T}} D_{\text{m}} \tilde{B}_{Cm} \, \text{d}\Omega \tag{37}$$

where

$$\tilde{B}_{CbI} = \frac{1}{A_C} \begin{bmatrix} 0 & 0 & 0 & 0 & \displaystyle\int_{\Gamma_C} N_I(\boldsymbol{x}) n_{Cx} \text{d}\Gamma & 0 \\[4mm] 0 & 0 & 0 & -\displaystyle\int_{\Gamma_C} N_I(\boldsymbol{x}) n_{Cy} \text{d}\Gamma & 0 & 0 \\[4mm] 0 & 0 & 0 & -\displaystyle\int_{\Gamma_C} N_I(\boldsymbol{x}) n_{Cx} \text{d}\Gamma & \displaystyle\int_{\Gamma_C} N_I(\boldsymbol{x}) n_{Cy} \text{d}\Gamma & 0 \end{bmatrix} \tag{38}$$

$$\tilde{B}_{mI} =$$

$$\frac{1}{A_C}\begin{bmatrix} \int\limits_{\Gamma_C} N_I(x)n_{Cx}d\Gamma & 0 & 0 & 0 & 0 & 0 \\ 0 & \int\limits_{\Gamma_C} N_I(x)n_{Cy}d\Gamma & 0 & 0 & 0 & 0 \\ \int\limits_{\Gamma_C} N_I(x)n_{Cy}d\Gamma & \int\limits_{\Gamma_C} N_I(x)n_{Cx}d\Gamma & 0 & 0 & 0 & 0 \end{bmatrix}$$

(39)

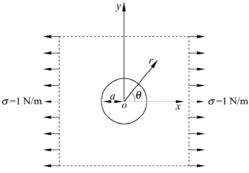$$\tilde{B}_{sI} = \begin{bmatrix} 0 & 0 & \dfrac{1}{A_e}\int\limits_{\Gamma_C} N_I(x)n_{Cx}d\Gamma & 0 & N_I(x) & 0 \\ 0 & 0 & \dfrac{1}{A_e}\int\limits_{\Gamma_C} N_I(x)n_{Cy}d\Gamma & -N_I(x) & 0 & 0 \end{bmatrix}$$

(40)

$$D_b = D_m = \frac{E}{1-v^2}\begin{bmatrix} 1 & v & 0 \\ v & 1 & 0 \\ 0 & 0 & \dfrac{1-v}{2} \end{bmatrix}$$

and

$$D_s = \begin{bmatrix} \mu & 0 \\ 0 & \mu \end{bmatrix} \qquad (41)$$

Because shell elements are oriented differently, a transformation matrix T needs to be used to transform the local matrices to the global matrices,

$$K^{global} = T^T K^{local} T, \quad F^{global} = T^T F^{local} \quad (42)$$

Scheme 3 of the SFEM for plate and shell problems uses SC>1 for the "bending" and "membrane" parts (for the shell) and SC=1 for the "shear" part which leads to a formulation which is free from shear locking. However, calculation of the "shear" part still uses Gauss integration to calculate $-N_I$ of $\tilde{B}_{sI}$, because the integration of $-N_I$ in the domain Ω cannot be transformed to a line integration on the boundary Γ_Ω. This may be one disadvantage of SFEM since the Gauss integration still has to be used for plate and shell problems.

3 Numerical Examples

3.1 Infinite plate with a circular hole

This example compares the efficiency of schemes 1 and 2 used in the SFEM and in the FEM for an incompressible locking problem.

Figure 1 represents a plate with a central circular hole, radius a=1 m, subjected to a unidirectional tensile load of $\sigma = 1$ N/m at infinity in the x-direction.

Fig. 1   Infinite plate with a circular hole subjected to unidirectional tension and the one quarter computational domain

Due to symmetry, only the upper right quadrant of the plate is modeled using 4-node elements as shown in Fig. 2. Plane strain condition is considered with $E = 1.0$ kN/m^2 and $v = 0.499\,999$. Symmetric conditions are imposed on the left and bottom edges and the inner boundary of the hole is traction free. The exact solution for the stress[12] is

$$\sigma_{11} = 1 - \frac{a^2}{r^2}\left[\frac{3}{2}\cos 2\theta + \cos 4\theta\right] + \frac{3a^4}{2r^4}\cos 4\theta,$$

$$\sigma_{22} = -\frac{a^2}{r^2}\left[\frac{1}{2}\cos 2\theta - \cos 4\theta\right] - \frac{3a^4}{2r^4}\cos 4\theta,$$

$$\tau_{12} = -\frac{a^2}{r^2}\left[\frac{1}{2}\sin 2\theta + \sin 4\theta\right] + \frac{3a^4}{2r^4}\sin 4\theta \quad (43)$$

where (r,θ) are the polar coordinates with θ measured counterclockwise from the positive x-axis. Traction boundary conditions are imposed on the right ($x = 5$) and top ($y = 5$) edges based on the exact

solutions Eq. (43). The displacement components corresponding to the stresses are

$$u_1 = \frac{a}{8\mu}\left[\frac{r}{a}(\kappa+1)\cos\theta + 2\frac{a}{r}\big((1+\kappa)\cos\theta + \cos 3\theta\big) - 2\frac{a^3}{r^3}\cos 3\theta\right],$$

$$u_2 = \frac{a}{8\mu}\left[\frac{r}{a}(\kappa-3)\sin\theta + 2\frac{a}{r}\big((1-\kappa)\sin\theta + \sin 3\theta\big) - 2\frac{a^3}{r^3}\sin 3\theta\right] \qquad (44)$$
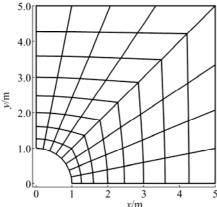

Fig. 2 Domain discretization of the infinite plate with a circular hole using 4-node elements

where $\mu = E/\big(2(1+\nu)\big)$ and κ is defined in terms of Poisson ratio as $\kappa = 3 - 4\nu$ for plane strain cases.

The following displacement error norm is used to examine the computed results.

$$e_{\mathrm{d}} = \sum_{i=1}^{n_{\mathrm{dof}}}\left|u_i - u_i^{\mathrm{h}}\right| \bigg/ \sum_{i=1}^{n_{\mathrm{dof}}}|u_i| \qquad (45)$$

where n_{dof} is the total number of degrees of freedom in the problem, u_i is the exact solution and u_i^{h} is the numerical solution.

Table 1 presents the strain energy, while Table 2 presents the displacement norm of the infinite plate for various meshes. The results show that both the FEM using full Gauss integration and the SFEM using SC=4 for all elements fail to give the correct results due to the incompressible locking, while both the SFEM and the FEM using schemes 1 and 2 overcome the incompressible locking phenomenon to give results that compare well to the exact solution. Comparison between the FEM and SFEM shows that the SFEM using schemes 1 and 2 gives better results than those of the FEM because the SFEM stiffness matrix is not as stiff as that of the FEM using full Gauss integration[6]. In addition, the results also show that scheme 2 gives better results than scheme 1.

Table 1 Strain energy $\frac{1}{2}u^{\mathrm{T}}P$ for the nearly incompressible case: $\nu = 0.499\ 999$ $\quad(\times 10^{-2})$

Mesh	SFEM (S1)	SFEM (S2)	FEM (S1)	FEM (S2)	SFEM (SC = 4)	FEM (4 Gauss)	Exact
4×4	0.9603	0.9620	0.9588	0.9609	0.9124	0.9123	0.9770
8×8	0.9738	0.9743	0.9733	0.9740	0.9213	0.9212	0.9770
12×12	0.9761	0.9763	0.9759	0.9761	0.9226	0.9225	0.9770

Table 2 Displacement norms of the infinite plate for the nearly incompressible case: $\nu = 0.499\ 999$ $\quad(\%)$

Mesh	SFEM (S1)	SFEM (S2)	FEM (S1)	FEM (S2)	SFEM (SC = 4)	FEM (4 Gauss)
4×4 (25 nodes)	1.87	1.81	2.08	1.84	15.98	15.98
8×8 (81 nodes)	0.42	0.39	0.50	0.40	16.73	16.73
12×12 (169 nodes)	0.17	0.16	0.20	0.16	17.30	17.30

3.2 Semi-infinite plate

This example also compares the efficiency of schemes

1 and 2 in the SFEM and in the FEM for an incompressible locking problem.

The semi-infinite plate shown in Fig. 3 is studied

subjected to a uniform pressure within a finite range ($-a \leqslant x \leqslant a$). The plane strain condition is considered. The analytical stresses are given by

$$\sigma_{11} = \frac{p}{2\pi}\big[2(\theta_1 - \theta_2)\big] - \sin 2\theta_1 + \sin 2\theta_2],$$

$$\sigma_{22} = \frac{p}{2\pi}\big[2(\theta_1 - \theta_2)\big] + \sin 2\theta_1 - \sin 2\theta_2],$$

$$\tau_{12} = \frac{p}{2\pi}\big[\cos 2\theta_1 - \cos 2\theta_2\big] \tag{46}$$

The directions of θ_1 and θ_2 are indicated in Fig. 3. The corresponding displacements can be expressed as

$$u_1 = \frac{p(1-v^2)}{\pi E}\begin{bmatrix} \dfrac{1-2v}{1-v}\big[(x+a)\theta_1 - (x-a)\theta_2\big] + \\ 2y\ln\dfrac{r_1}{r_2} \end{bmatrix},$$

$$u_2 = \frac{p(1-v^2)}{\pi E}\begin{bmatrix} \dfrac{1-2v}{1-v}\Big[y(\theta_1-\theta_2) + 2H\arctan\dfrac{1}{c}\Big] + \\ 2(x-a)\ln r_2 - 2(x+a)\ln r_1 + \\ 4a\ln a + 2a\ln(1+c^2) \end{bmatrix} \tag{47}$$

where $H = ca$ is the distance from the origin to point O', the vertical displacement is assumed to be zero and c is a coefficient.
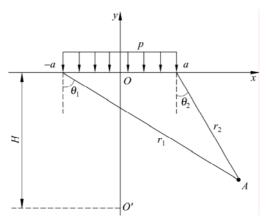

Fig. 3 Semi-infinite plate subjected to a uniform pressure

Due to the symmetry about the *y*-axis, the problem is modeled with a $5a \times 5a$ square with $a = 0.2$ m, $c = 100$, and $p = 1$ MPa. The left and bottom sides are constrained using the exact displacements given by Eq. (47) while the right side is subjected to tractions computed from Eq. (46). The domain is discretized as shown in Fig. 4. Four smoothing cells are used for

each element. The displacement norm is given in Eq. (45) and the energy norm is defined as

$$e_e = \frac{1}{2}\left[\int_\Omega (\varepsilon^h - \varepsilon)^T D(\varepsilon^h - \varepsilon)d\Omega\right]^{1/2} \tag{48}$$
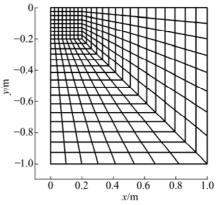

Fig. 4 Domain discretization of the semi-infinite plate using 4-node elements

Table 3 presents the displacement norm, while Table 4 presents the energy norm of the semi-infinite plate for various meshes. The results again show that both the FEM using full Gauss integration and the SFEM using SC=4 for all elements fail to give correct results due to the incompressible locking, while both the SFEM and the FEM using schemes 1 and 2 overcome the incompressible locking phenomenon to give results that compare well to the exact solution. Comparison of the FEM and the SFEM shows that the SFEM using schemes 1 and 2 gives better results than the FEM. In addition, the results also show that scheme 2 gives better results than scheme 1. This along with its general applicability ensures wide application of scheme 2 for incompressible locking problems.

3.3 Square plate subjected to a concentrated load at the center[11]

This example shows that the SFEM with scheme 3 overcomes shear locking in a plate problem.

A simply supported square plate is subjected to a concentrated load at the center. The plate is the side lenth $a = 25.4$ cm and its thickness t changes from 0.127 cm to 5.08 cm. The plate is made of the steel whose elastic modulus $E = 206.84 \times 10^6$ kPa and Poisson ratio is 0.3. The applied force is 177.93 N at the center. A quarter of the plate is modeled due to symmetry and it is divided into sixteen 4-node elements as shown in Fig. 5.

Table 3   Displacement norm of the semi-infinite plate for the nearly incompressible case: $\nu = 0.499\ 999$ (%)

Mesh	SFEM (S1)	SFEM (S2)	FEM (S1)	FEM (S2)	SFEM (SC = 4)	FEM (4 Gauss)
97	0.480	0.460	0.500	0.470	14.10	14.12
353	0.120	0.110	0.130	0.120	13.71	13.76
769	0.051	0.049	0.056	0.051	13.55	13.64
1345	0.030	0.029	0.032	0.030	13.44	13.55

Table 4   Energy norm for the nearly incompressible case: $\nu = 0.499\ 999$

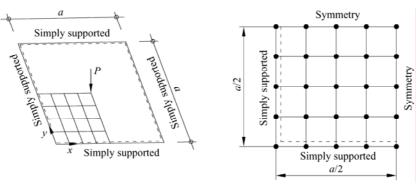| Mesh	SFEM (S1)	SFEM (S2)	FEM (S1)	FEM (S2)	SFEM (SC = 4)	FEM (4 Gauss)
97	21.55	21.29	21.93	21.47	591.18	2999.64
353	9.62	9.44	9.82	9.56	327.00	1761.61
769	5.97	5.87	6.09	5.94	284.76	1259.26
1345	4.29	4.20	4.33	4.24	268.61	990.50

Fig. 5   Square plate subjected to transverse loading and its quarter model

The analytical solution for the deformation at the center[13] is

$$w_{max} = 0.0116 \frac{Pa^2}{D} \tag{49}$$

where P is the applied load at the center and $D = \dfrac{Et^3}{12(1-\nu^2)}$.

Figure 6 presents the normalized displacement $\dfrac{wD}{Pa^2}$ at the center versus the thickness. The results show that the FEM using full Gauss integration and the SFEM using SC=4 for all bending and shearing parts give divergent results as the plate thickness is reduced due to shear locking. However, the SFEM and the FEM both using scheme 3 give results that converge to that of the thin plate as the plate thickness is reduced.

3.4   Barrel vault shell subjected to its own weight[11]

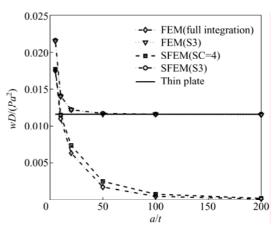This example shows that the SFEM with scheme 3

Fig. 6   Displacement at the center versus the thickness parameter

overcomes shear locking in a shell problem.

The barrel vault has a radius of 7.62 m, subtended angle of 80°, length of 15.24 m, and thickness of 7.62 cm. The structure has an elastic modulus of $E = 20.684$ GPa, Poisson ratio of 0, and weight of 5.382 kg/m². The two curved edges are assumed to be

supported by rigid diaphragms and the other two edges are free. Because of symmetry, only a quarter of the structure is modeled as shown in Fig. 7. The analytical solution for the vertical deflection of the middle of the free side is 9.406 cm[14].

Table 5 lists the vertical deflection at the middle of the free edge. The results show that both the FEM using full Gauss integration and the SFEM using SC=4 for all bending, membrane, and shearing fail to give the correct results due to shear locking, while the SFEM and the FEM both using scheme 3 overcome this shear locking to give good results. Moreover, the SFEM result is better than that of the FEM due to the smaller stiffness of the SFEM matrix.
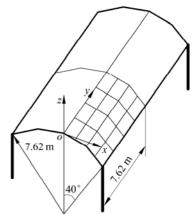

Fig. 7   Barrel vault with discretization scheme

Table 5   Vertical deflection at the middle of the free edge   (cm)

Mesh	FEM (S3)	SFEM (S3)	FEM (Full Gauss integration)	SFEM SC=4 for all bending and shearing	Analytical solution
4×4	8.912	9.396	0.402	0.523	9.406

4   Conclusions

This paper describes three selective SFEM schemes. The formulation and numerical examples show that the SFEM can efficiently solve problems with incompressible locking and shear locking by splitting the strain energy into parts and applying different numbers of smoothing cells to these parts in calculating the stiffness matrix. The SFEM works well for 2-dimensional elasticity problems because the strain gradient matrix has only derivatives of the shape functions and integration on the domain can be transformed to line integration on the boundary. However, for plate and shell problems, because the strain gradient matrix of the shear part $\tilde{\boldsymbol{B}}_s$ includes the shape functions themselves, the integration of the shape functions on the domain can not be transformed to line integration on the boundary. Therefore, the line integration is used in the SFEM for the derivatives of the shape functions, and the Gauss integration is used for the shape functions themselves.

SFEM schemes 1 and 2 are both free from nearly incompressible locking, but scheme 2 is more general and gives better results than scheme 1. Scheme 2 can be applied for anisotropic and nonlinear situations, while scheme 1 can only be applied for isotropic and linear situations. SFEM scheme 3 is free from shear locking and can be applied to plate and shell problems.

In general, the SFEM with the three schemes, scheme 1, scheme 2, and scheme 3, gives better results than the FEM with these schemes mainly because the SFEM stiffness matrix is not as stiff as that of the FEM using full Gauss integration[6].

References

[1]   Zienkiewicz O C, Taylor R L, Too J M. Reduced integration technique in general analysis of plates and shells. *International Journal for Numerical Methods in Engineering*, 1971, **3**: 275-290.

[2]   Malkus D S, Hughes T J R. Mixed finite element methods-reduced and selective integration techniques: A unification of concepts. *Comp. Meth. Appl. Mech. Engng.*, 1978, **15:** 63-81.

[3]   Hughes T J R. The Finite Element Method: Linear Static and Dynamic Finite Element Analysis. New York: Prentice-Hall, 1987.

[4]   Hughes T J R. Generalization of selective integration procedures to anisotropic and nonlinear media. *International Journal for Numerical Methods in Engineering*, 1980, **15**: 1413-1418.

[5]   Liu G R, Dai K Y, Nguyen T T. A smoothed finite element method for mechanics problems. *Computational Mechanics*, 2007, **39**: 859-877.

[6] Liu G R, Nguyen T T, Dai K Y, Lam K Y. Theoretical aspects of the smoothed finite element method (SFEM). *International Journal for Numerical Methods in Engineering*, (in press, published on line on 29 December 2006).

[7] Bathe K J. Finite Element Procedures. Englewood Cliffs, NJ: Prentice Hall, 1996.

[8] Liu G R, Quek S S. The Finite Element Method: A Practical Course. Oxford: Butterworth Heinemann, 2003.

[9] Zienkiewicz O C, Taylor R L. The Finite Element Method, 5th ed. Oxford: Butterworth Heinemann, 2000.

[10] Commend S, Truty A, Zimmermann T. Stabilized finite elements applied to elastoplasticity: I. Mixed displacement-pressure formulation. *Computer Methods in Applied Mechanics and Engineering*, 2004, **193**: 3559-3586.

[11] Kwon Y W, Bang H. The Finite Element Method Using Matlab. CRC Press LLC, 2000.

[12] Timoshenko S P, Goodier J N. Theory of Elasticity, 3rd ed. New York: McGraw-Hill, 1970.

[13] Ansel C U. Stresses in Plates and Shells. Singapore: McGraw-Hill, 1999.

[14] Ashwell D G. Strain elements, with applications to arches, rings and cylindrical shells. In: Ashwell D G, Gallagher R H, eds. Finite Elements for Thin Shells and Curved Members. London: Wiley & Sons, 1976: 91-111.

2007 English Summer Camp Opens

Tsinghua launched its fourth English Summer Camp on July 9, 2007 for nearly 3200 students who have just completed their freshman year.

The English Summer Camp features a flexible learning style, the students can choose from four ways of learning. The four learning styles include intensive training in listening and speaking, comprehensive knowledge training, internet self-study, and overseas studies.

A series of activities including lectures, singing competition, movies, dance, and Camp Store will be held to help the students learn more about foreign cultures.

More than 130 foreign teachers and foreign volunteers took part in the camp.

（From http://news.tsinghua.edu.cn，2007-07-13）